Limnol. Oceanogr., 37(3), 1992, 501–509

A spectral model of the beam attenuation coefficient in the ocean and coastal areas

Kenneth J. Voss
Department of Physics, University of Miami, Coral Gables, Florida 33124

Abstract

A large set (~100 data points at each wavelength) of multispectral beam attenuation, $c(\lambda)$, data at nine wavelengths (440, 450, 490, 520, 535, 550, 565, 630, and 670 nm) is used to develop a spectral model of the beam attenuation coefficient. The relationship $c(\lambda) - cW(\lambda) = [c(490\text{ nm}) - cW(490\text{ nm})](1.563 - 1.149 \times 10^{-3}\,\lambda)$ describes the spectral variation of $c(\lambda)$ where $cW(\lambda)$ is the pure water beam attenuation and λ is the wavelength in nm. From a subset of the data a relationship of chloropyll (Chl) to $c(490)$ was found to be $c(490) = 0.39\,\text{Chl}^{0.57}$; however there is significant scatter in this relationship. The spectral c model was tested with independent data sets and the average percent difference of the measured to predicted values ranged from 0.4 to 5% for the different spectral bands.

The spectral beam attenuation coefficient c is an important property in optical oceanography. Because c (units given in list of notation) is an inherent optical property (Preisendorfer 1976) it is an important measurement in the optical characterization of a water sample. The inverse of the beam attenuation coefficient, the attenuation length, is important as a scaling parameter for problems in imaging and radiative transfer. When calibrated correctly, c can be used to determine the suspended particulate load in a water sample.

Reported measurements of c have predominantly been in a single spectral band. Most often the photopic band has been used (with an instrument such as the Martek transmissometer) or more recently in a spectral band at 660 nm (with an instrument such as the SeaTech transmissometer). Comparisons between data sets of c in different spectral bands require knowledge of the spectral nature of $c(\lambda)$. Previous studies, in which measurements at multiple wavelengths were reported, were of phytoplankton cultures (Bricaud et al. 1983) or for cases of limited geographic extent (Kitchen et al. 1982). The goal of this work was to investigate a large, geographically diverse, data set and empirically determine the spectral characteristics of $c(\lambda)$. $c(\lambda)$ will be shown to have a simple wavelength dependence that appears to be broadly applicable. This simple dependence allows measurements at one wavelength to be extrapolated to other spectral bands.

Definitions

c is defined as "the attenuance of an infinitesimally thick layer of the medium normal to the beam, divided by the thickness of the layer" (Morel and Smith 1982). In simpler terms it is simply a measure of the attenuation of a beam of light due to scattering and absorption. For a homogeneous medium of finite thickness, c is defined as

$$c = -\ln(\Delta L)/d$$

where ΔL is the change in radiance along a path of length d. These measurements are typically made with a beam transmissometer which measures the change in transmission (T) over its pathlength (d) due to water. These instruments are calibrated by two methods. The first involves setting the transmission of the optical path in air to a calibration value (T_{air}, which can be easily calculated) and measuring the transmission in water (T_w). c is then

Acknowledgments

I thank Dennis Clark for allowing me to use the NOAA spectral attenuation data. I also thank Roswell Austin, Albert Chapin, Gerald Edwards, and Jeffrey Nolten for collecting the Vislab data set, and Leonard Lopez for collating the data. I am also grateful to Andre Morel and Howard Gordon for their many suggestions.

This work was supported by the Applied Physics Laboratory/Johns Hopkins University and the Ocean Optics program of the Office of Naval Research contract N00014-90-J-1505.

Notation

a	Absorption coefficient, m^{-1}
b	Total scattering coefficient, m^{-1}
$c(\lambda)$	Spectral beam attenuation coefficient, m^{-1}
$cW(\lambda)$	Spectral beam attenuation coefficient of pure water, m^{-1}
$c - cW(\lambda)$	$=c(\lambda) - cW(\lambda)$, m^{-1}
Chl	Chlorophyll concn, mg m^{-3}
d	Sample pathlength of transmissometer, m
γ	Junge size distribution exponent
λ	Wavelength of light, nm
n	Real part of the index of refraction
n'	Imaginary part of the index of refraction
N	Number of particles per unit volume, ml^{-1}
r	Particle radius, m
T	Transmission
T_{air}	Transmission of transmissometer in air
T_w	Transmission of transmissometer in water

$$c = -\ln(T_w)/d.$$

In the second method the transmissometer is immersed in a standard and the transmission is set to the known transmittance of this standard.

Beer's law describes the change in c with concentration, and as a consequence c can be separated into components due to scattering (b) and absorption (a):

$$c = a + b.$$

c can also be broken apart into its constituent parts:

$$c_{\text{total}} = c_{\text{water}} + c_{\text{particles}} + c_{\text{dissolved materials}}.$$

The constituent parts of c_{total} can, to a certain extent, be broken into absorption and scattering portions, with the reservation that for particulates, changes in the absorption properties can affect the total scattering coefficient, i.e. scattering and absorption may not be independent processes (Mueller 1973). Although the units of c do not explicitly illustrate it, the beam attenuation for most materials is dependent on wavelength through variations in absorption and scattering. Throughout this paper I make use of separability and subtract the pure water component [$cW(\lambda)$] from the measured c, i.e.

$$c - cW(\lambda) = c(\lambda) - cW(\lambda).$$

The scattering and absorption of pure water is highly wavelength-dependent (illustrated by Smith and Baker 1981), hence removing this predictable spectral dependence allows the remaining portion to be analyzed more simply.

Data presentation

Data used in this report were compiled from several cruises during 1975–1989, covering a wide range of oceanic and coastal conditions and locations. Figure 1 shows the approximate locations of stations from which data were obtained. They include stations in the North Atlantic, North Pacific, Gulf of Mexico, and Greenland Sea.

The data were acquired with two instruments of similar construction. The first was the Visibility Laboratory spectral transmissometer (VLST), a transmissometer with a cylindrically limited optical system (Petzold and Austin 1968). An important characteristic of this transmissometer is that the exit aperture of the source is focused on the field stop of the receiver, while the field stop of the source is imaged on the entrance aperture of the detector. The end result is that in the absence of scattering all of the source illumination falls on the receiver aperture. And, with or without scattering, the receiver accepts any flux that falls on its entrance aperture from the direction of the source exit aperture. This transmissometer has a maximum acceptance angle of ~2.3° (accepts 2.3° of forward-scattered flux), however this scattering angle is only relevant for the exact center of the transmissometer and for only a limited amount of the source flux. The error in the beam attenuation derived from this transmission measurement is ~10%, with little spectral variation (results of an unpublished study of the VLST using Monte-Carlo modeling and a data base of small-angle scattering data). This transmissometer is similar to the Martek transmissometer except that the VLST has been modified to allow spectral filters to be placed in the optical path, allowing measurement of the beam attenuation in five spectral bands (440, 490, 520, 550, and 670 nm). Data were also obtained with another transmissometer of the same design but with different spectral filters (450, 490, 535, 565,

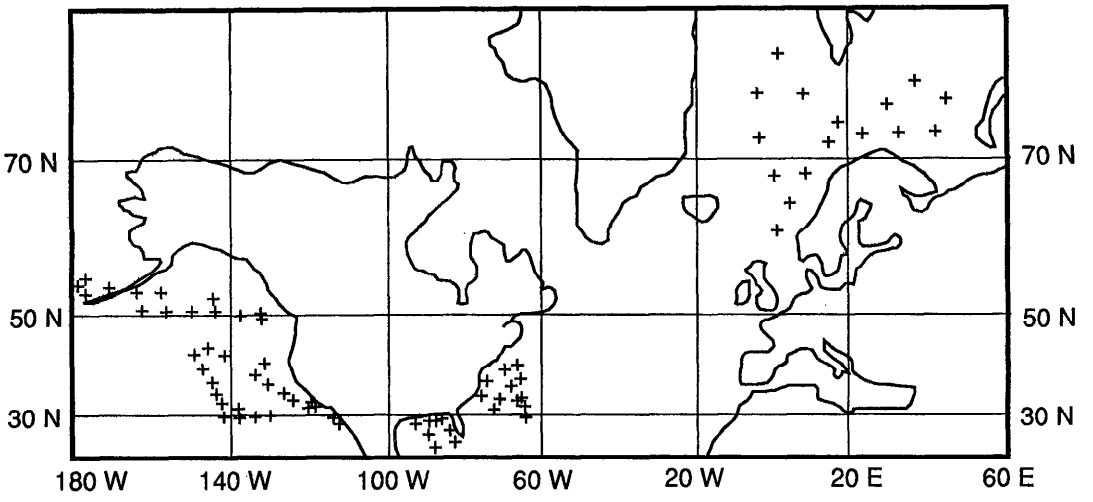

Fig. 1. Chart indicating geographic locations of stations. Symbols (+) mark locations at which data were obtained.

and 630 nm) fielded by Dennis Clark (NOAA). Both of these transmissometers have a 1-m sample pathlength. The data obtained with the VLST will be referred to as the Vislab data set and that obtained with the other transmissometer as the NOAA data set. I restricted the study to only these two instruments to decrease possible errors due to varying acceptance angle and optical design on the resultant empirical relationships. No effort was made to correct for the finite acceptance angle of the transmissometers. The finite acceptance angle has been was found to cause little (<2%) spectral variation in the measured $c(\lambda)$. Additionally the model is tested with measurements obtained with a transmissometer of a very different optical design to illustrate the transportability of this model to other transmissometers.

The transmissometers used do not measure c for all wavelengths simultaneously, but must have the spectral filters sequentially inserted into the optical path. Because of this, the common mode of operation is sequential casts through the water column (0–200 m) with each filter as rapidly as possible. Passage of internal waves and ship movement during the measurement period can cause errors in collating the data obtained during the separate casts due to data aliasing. Standard procedures to correct for these effects, such as indexing the data with water density rather than depth, depend on having information on the salinity profile (used in calculating the density profile), which was not available. Data were thus carefully selected to reduce these errors. The selection process involved selecting depths at which the beam attenuation was relatively constant or which were identifiable (the particulate maximum). Even with these efforts some mismatches undoubtedly remain and could account for some of the variability in the results obtained. Portions of the Vislab data set were obtained in a manner that reduced these aliasing effects. Specifically the instrument was held at a given depth, and measurements for each wavelength were obtained in rapid succession. In this manner the measurements of the five wavelengths were closely correlated and aliasing effects could be neglected.

Figures 2–4 illustrate the $c - cW(\lambda)$ vs. $c - cW(490)$ where the pure water c is detailed by Smith and Baker (1981). I chose 490 nm as the reference wavelength for two reasons: first, it is the wavelength on which the spectral K model of Austin and Petzold (1986) is referenced; second, the data exist at this wavelength for both the Vislab and the NOAA data set. The regression coefficients are listed in Table 1 along with the relevant regression statistics. As one can see

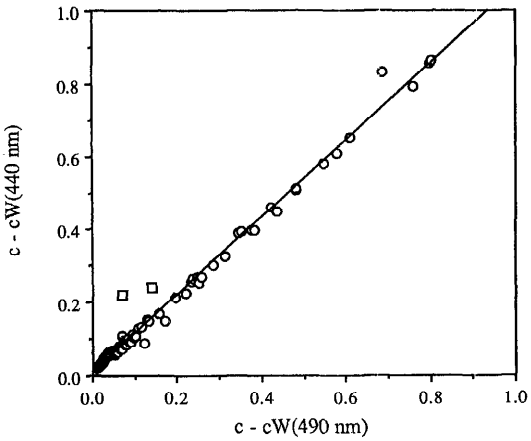

Fig. 2. Plot of $c - cW(440)$ vs. $c - cW(490)$. O—Data points used in regression analysis; line is least-squares fit to data. □—Points excluded from analysis because of anomalously high $c - cW(440)$ values. Units of the axes are m^{-1}.

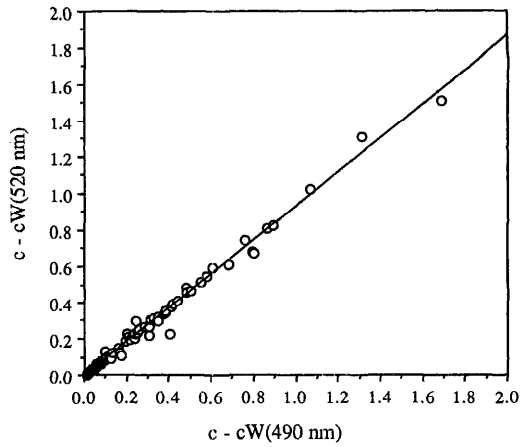

Fig. 4. Plot of $c - cW(520)$ vs. $c - cW(490)$. O—Data points; line is least-squares fit to data. Typical of regressions for wavelengths >490 nm. Units of the axes are m^{-1}.

the regressions are very good: the worst r^2 value is 0.92 with several values of 0.99.

The intercepts of these regressions were not 0. For five of the regressions (440, 450, 520, 535, and 550 nm) intercepts were ≤ 0.01 m^{-1}. The source of this intercept could be small errors in calibration of the instrument, where an intercept of this magnitude could be caused by incorrect setting of the T_{air} by 1% or less. An alternative explanation would be due to errors in the derived cW. The offset for 630 and 670 nm is <20% of the pure water value of Smith and Baker (1981)—within the reported spread of their measurements. The magnitude of the offset for 565 nm is more difficult to explain and at this point is not understood.

Two data points from the Vislab data set and 10 in the NOAA data set were excluded from the regressions, but are shown in Figs. 2 and 3. The 10 data points in the NOAA data set were from about the same location (De Soto Canyon, Gulf of Mexico, 30°N, 87°W) and the same season (October–November), but were taken in two different years. These points distinguish themselves by lying far above the other data points. A regression performed on these 10 points alone results in a slope within 0.3% of the general line but offset by 0.20 m^{-1}. This offset indicates a background concentration of some absorbing or scattering agent that did not covary with the other particulates and was more effective at 440 nm than at 490 nm. The other feature was that these

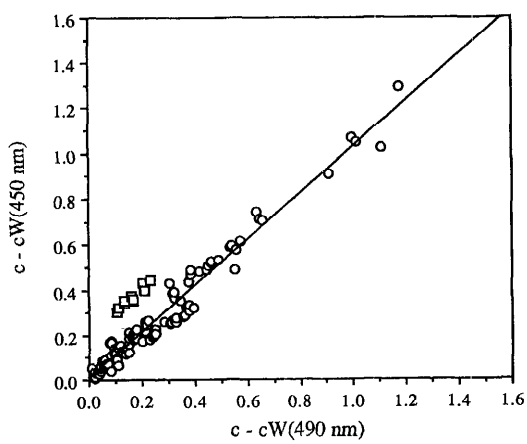

Fig. 3. As Fig. 2, but of $c - cW(450)$ vs. $c - cW(490)$.

Table 1. Results of regressions of $c - cW(\lambda)$ and $c - cW(490)$ using the accumulated data set.

Wavelength (nm)	Slope	Offset	r^2	s_b	No. of points
440	1.059	0.0080	0.995	0.008	89
450	1.014	0.0085	0.956	0.019	112
490	1.000				
520	0.933	−0.0066	0.991	0.009	106
535	0.900	−0.0021	0.922	0.025	112
550	0.935	−0.012	0.988	0.010	101
565	0.844	0.055	0.931	0.022	112
630	0.805	−0.051	0.955	0.017	112
670	0.850	−0.032	0.961	0.017	101

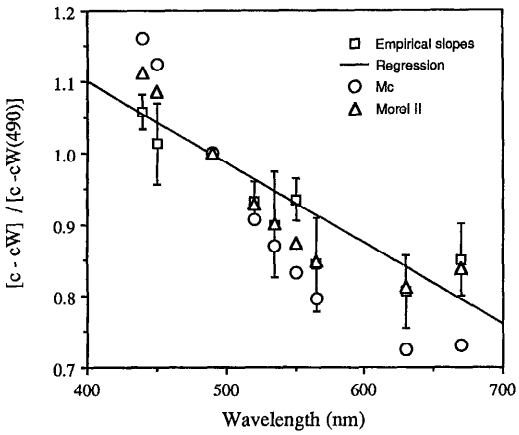

Fig. 5. Regression slopes vs. wavelength. Line is a weighted least-squares fit to the slopes. Error bars are ±1 SD in the slope values. Also shown are the slopes derived from Morel and Gentili (1991), shown as Mc, and my modification of the model (reduced wavelength dependence on the scattering), shown as Morel II.

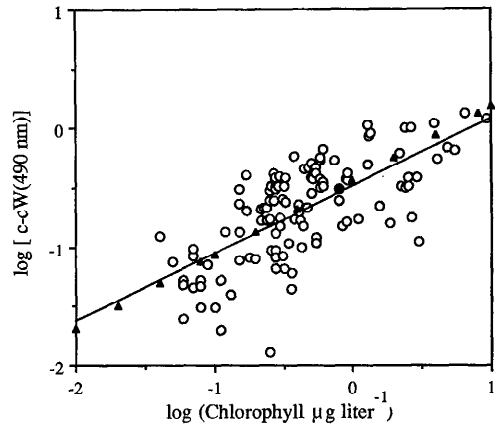

Fig. 6. Chlorophyll dependence of $c - cW(490)$. O—Data points from this data set; ▲—derived from the model of Morel and Gentili (1991). Line is least-squares fit to data.

points did not distinguish themselves at wavelengths >490 nm. These facts indicate that the cause of this offset was probably an anomalously large concentration of dissolved materials. It is interesting that this occurred in two successive years at about the same concentration (evidenced by the same offset). The two data points excluded in the Vislab set also had anomalously large $c - cW(440)$, but were from a different location (off Bermuda). The offset in this case was much smaller ($\sim 0.1\ m^{-1}$) but obviously did not have the same relationship as the rest of the curve.

The slopes found with these regressions are shown, with error bars, in Fig. 5. Another similar model of the beam attenuation coefficient can be constructed by combining the $b(\lambda, \text{Chl})$ and the $a(\lambda, \text{Chl})$ model of Morel and Gentili (1991) (hereafter referred to as Mc), where Chl is the chlorophyll concentration. The results for this model are also shown in Fig. 5. This model is specifically for case 1 waters (Morel and Prieur 1977)—waters for which phytoplankton are the dominant influence. I selected out the case 1 portion of the data base and found that there was very little difference in the spectral c relationship. The original model by Morel and Gentili predicted a scattering function that was inversely proportional to wavelength. When the spectral dependence of the scattering was changed from $(\lambda/550\ \text{nm})^{-1}$ to $(\lambda/550\ \text{nm})^{-0.5}$ the model marked as Morel II in Fig. 5 was obtained. As can be seen the agreement is significantly better except in the blue wavelengths where it is still quite reasonable.

I also looked at the variation of $c(490)$ with chlorophyll. I did not have chlorophyll data for the entire data set, so I used a subset for which contemporaneous data existed (Shapiro 1986; Shapiro and Haugen 1986). In Fig. 6 these data are plotted along with sample points resulting from the Mc. The data fit the line

$$c(490) = 0.39\ \text{Chl}^{0.57}.$$

As can be seen there is a lot of scatter in these data. The spread of values is in line with the variability in the $b(\lambda)$ vs. Chl relationships shown by Gordon and Morel (1983). Kitchen and Zaneveld (1990) have also shown a decoupling of chlorophyll and beam attenuation in in situ measurements. This fit to the line is not significantly different from the relationship predicted by Mc as shown in Fig. 6.

Test of the model

Three examples are used as independent tests of this spectral model. First, an independent data set obtained with the VLST located in the near-coastal Pacific off San Diego (33°04.7′N, 118°15.08′W, 5 April 1989) was used. Few data points in the orig-

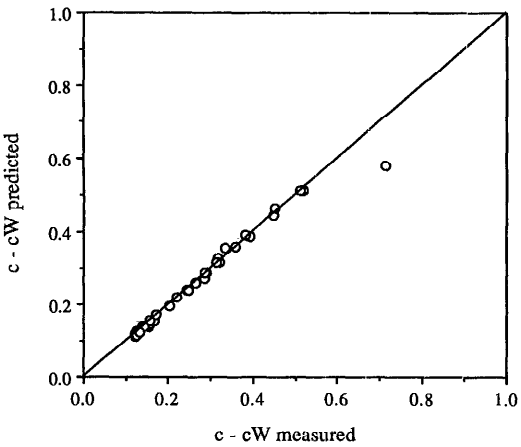

Fig. 7. Plot of measured vs. predicted $c - cW(\lambda)$ for an independent data set in the near-coastal eastern Pacific Ocean. Line indicates a perfect fit. This figure illustrates success of the model in predicting spectral variation.

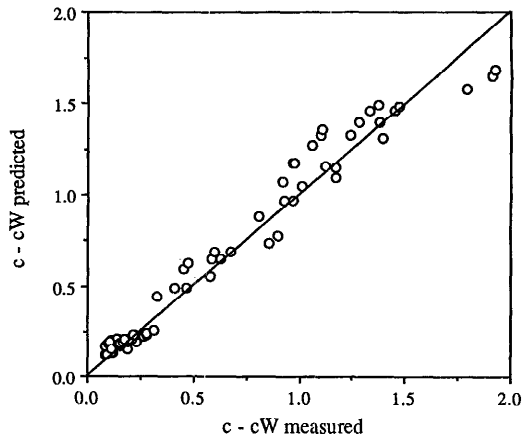

Fig. 8. Plot of measured vs. predicted $c - cW(\lambda)$ for a station in a coccolithophore bloom in the Gulf of Maine. Line indicates a perfect fit. This figure illustrates failure of the model in a single-species bloom.

inal data set were from this area; thus it should be a good test of the general applicability of the relationships. Data were obtained with the VLST for nine depths for which $c - cW(490\text{ nm})$ varied from 0.13 to 0.55 m^{-1}. The values of $c - cW(490\text{ nm})$ were then used to predict $c - cW(\lambda)$ and these predictions compared to the measured values. For example, the $c - cW(520\text{ nm})$ relationship used was simply

$$\begin{aligned} c - cW(520)_{\text{pred}} &= c(520) - cW(520) \\ &= 0.933\,[c(490) - cW(490)]. \end{aligned}$$

Figure 7 is a plot of the measured vs. predicted values of $c - cW(\lambda)$, and Table 2 illustrates the statistics of the percent error $\{100 \times [c - cW(\lambda)_{\text{pred}} - c - cW(\lambda)_{\text{meas}}]/[c - cW(\lambda)_{\text{meas}}]\}$. The predictions are very good: the average percent error ranges from 0.4 to 5.5%, with a standard deviation that ranges from 1.4 to 6.3. The maximum error was 18%.

Table 2. Results of applying the model to an independent data set obtained with the VLST. Values shown are the percent difference.

Wavelength (nm)	Mean	SD	Variance	Max
440	5.5	6.3	4.0	18
520	0.41	1.4	1.9	2.0
550	0.86	2.1	4.2	4.4
670	1.6	4.1	25	8.9

These predictions are based on an average resultant from the many stations contained in the above regressions, so specific instances can be found for which the coefficients are not valid. Specifically, cases where a single phytoplankton species dominates, such as during a bloom, would not necessarily follow the above relationships.

Second, as an extreme example, the above model was used to predict values of $c - cW(\lambda)$ given measurements of $c(490\text{ nm})$ obtained during a coccolithophore bloom. Figure 8 is the measured vs. predicted values of $c - cW(\lambda)$, and Table 3, part a details the statistics of the percent error. Somewhat surprisingly the predictions work fairly well even in this area where one might expect

Table 3. Results of applying the model to a data set obtained in a coccolithophore bloom. Part a is the entire data set; part b excludes a single station from the data set. Values shown are the percent difference.

Wavelength (nm)	Mean	SD	Variance	Max
a. Entire data set				
440	8.3	9.4	88.1	21
520	−10.7	15.2	230	45
550	−20.5	20.5	420	77
670	23.2	37.8	1,430	102.1
b. Excluding one station				
440	10.6	8.4	70	21
520	−4.7	6.2	38	21
550	−12.6	7.5	57	34
670	23.6	10.9	119	46

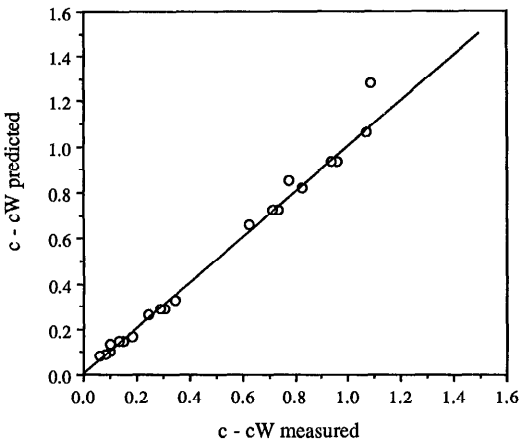

Fig. 9. Plot of measured vs. predicted $c - cW(\lambda)$ for a diverse data set obtained with another type of transmissometer (ALSCAT). Line indicates a perfect fit. This figure illustrates ability of the model to work with transmissometers of varied design.

major problems. These stations were in the middle of an extremely strong bloom of *Emiliania huxleyi*—so strong that the water turned turquois due to the intense scattering of the coccoliths (more information on this bloom is given by Balch et al. 1991). The predictions work fairly well even to $c - cW$ values of 1.6 m^{-1}. The statistics of the percent difference (Table 3) show that there is more error in the prediction than in the previous case; however, the average error is still only 8–23%.

The maximum errors are large, ranging from 21 to 102%, but much of the error and variance is due to just three points which were all from the same station (exhibiting very high surface coccolith counts) at depths below the particulate maximum. The c values were not extremely high or low [$c - cW$(490 nm) = 0.214, 0.195, 0.222 m^{-1}]; however, the error in each case was a prediction of higher $c - cW(\lambda)$ for all the wavelengths >490 nm, i.e. c(490 nm) used in the predictions was anomalously higher than $c(\lambda)$ at these wavelengths. Detrital absorption signatures indicate a strong inverse relationship with wavelength (Iturriaga and Siegel 1988) which could affect c to some extent, hence these data points could contain an anomalously large amount of detrital material. Table 3b contains the statistics for the test case when these three data points are removed. The average error, standard deviation of the error, and maximum error all decrease with removal of these three points for the wavelengths >490 nm, although they do not change significantly for c(440 nm).

Table 4. Results of applying the model to an independent data set obtained with the ALSCAT. Values shown are the percent difference.

Wavelength (nm)	Mean	SD	Variance	Max
440	3.3	3.4	11	−8.6
520	−1.2	3.4	11	−4.8
550	3.5	4.1	17	8.7
670	16.9	11.6	136	33

Third, a data set was compiled of spectral transmission data obtained with a collimated beam transmissometer. This transmissometer, ALSCAT (Austin and Petzold 1975), has a very small angular acceptance of 0.09 degrees and is a collimated beam design. The data were a diverse set of stations in the Pacific, Atlantic, and Gulf of Mexico. The above model was used with the 490-nm data and compared with the measured values of $c - cW(\lambda)$. The results are shown in Fig. 9; Table 4 details the comparison. The model did a very good job of predicting the spectral variation of $c(\lambda)$ with a degradation of the performance at 670 nm. The points above the line in Fig. 9 were all at 670 nm. The spectral model is relatively insensitive to the transmissometer design, thus showing the general applicability of the model.

Dissolved material—One factor which has come under increased scrutiny lately is the role of dissolved materials (DM) in determining the optical proprieties of the open ocean (Roesler et al. 1989). If DM were an important component in the data obtained in this study, its effects would be most evident in the blue wavelengths, particularly at 440 nm. If the concentration of DM covaried with the particulate load, one would not be able to discriminate this effect from the other contributions to c. If the concentration of DM did not covary with the other particulates, it would be indicated by a decreased correlation between c(490 nm) and c(440 nm) when compared to other wavelengths. The figures and tables show that it does not occur. Thus DM, if significant, ap-

pears to covary with particulates in this data set, with the exception of the points described previously. It is interesting to note how rarely it occurs and how these points stand out from the rest of the data set.

Size distribution—Previous work (Diehl and Hardt 1980) has suggested that the spectral dependence of the beam attenuation would have a simple wavelength dependence for the case of a Junge-type particle size distribution ($N \propto r^{-\gamma}$, where N is the number of particles and r is the particle diameter). This dependence can be shown to be $c(\lambda) \propto \lambda^{3-\lambda}$. Kitchen et al. (1982) found, with measured $c(\lambda)$ and size distribution data, that this relationship was not so simple. They found that the slope of the size distribution was correlated with the spectral shape of c, with measurements of $c(450\text{ nm})$ extending from 0.2 to 3 m^{-1}. Closer examination of their figure 4 shows that the size distribution seemed to have a significant effect only in waters for which $c(450\text{ nm}) > 1\ m^{-1}$, even when the slope of the size distribution (γ) varied from 2.8 to 4.4. When $c(450)$ is restricted to values $<1\ m^{-1}$, our relationship fits their data quite well, regardless of size distribution. This fit suggests that the consistency of our spectral relationship does not imply some "universal" or statistically significant size distribution, but must be independent of the size distribution.

Other wavelengths—Although the beam attenuation can be broken into the scattering and absorption components, it is somewhat misleading in the case of $c_{\text{particles}}$ because scattering and absorption are not independent. b, c, and a can be calculated for spherical particles using approximations given by Van de Hulst (1981), assuming a refractive index (n) approximately the same as water (the n for marine particulates is thought to be around 1.05 times the refractive index of water, Gordon and Brown 1972). Morel and Bricaud (1981) have shown how b and a vary with changes in n', the imaginary part of the particle index of refraction (related to the absorption coefficient for the particle). In general b does not remain constant with varying n'; in fact if one looks at specific regions of b, there are areas in which it increases with larger n' because destructively interfering diffracted light is absorbed and areas where it decreases as constructively interfering light is absorbed. There is also an effect in absorbing materials caused by anomalous dispersion, which causes the real index of refraction to vary around strong absorption bands in materials and hence changes b. All of these factors have been shown to reduce the effect of the absorption bands (Mueller 1973; Bricaud et al. 1983) on the extinction coefficient.

Most measurements of the spectral beam attenuation of phytoplankton cultures (Bricaud and Morel 1986; Bricaud et al. 1983), using instruments with small forward scattering acceptance angles, exhibit a linear relationship with wavelength. Figure 5 showed the data for the slopes along with the error in the slope values (± 1 SD) derived from the data. A weighted least-squares fit to these data has been performed and is shown in Fig. 8. This line is described by

$$c - cW(\lambda) = c - cW(490)(1.563 - 1.149 \times 10^{-3}\lambda)$$

(where λ is in nm). The scatter about the line, particularly with 670 nm being above the line and 550 and 635 nm below the line, seems to indicate an influence by phytoplankton pigments. However 440 and 450 nm, which should be most noticeably affected in this case, are not significantly different from the line. Even the variation of the 670-nm point from the line is not large when taken in the context of total c. For example if the line fit is used to determine $c(670)$ when $c(490) = 0.6\ m^{-1}$ (a large beam attenuation value) $c(670)$ is 0.92 m^{-1} which differs only by 4% from the value obtained with the point regression found in this study. Because no clear picture emerges indicating that c either should be or is affected by phytoplankton pigments and, as indicated earlier, most studies have shown linear spectral beam attenuation values, I feel the line is the most reasonable interpolation of the data.

An alternative model would be to use the model detailed by Morel and Gentili (1991) with two caveats. First, the wavelength dependence of the scattering component fits the data at wavelengths >490 nm with an exponent of -0.5 (instead of -1.0). Second,

at wavelengths <490 nm, this model predicts a $c - cW(1)/c - cW(490)$ that is slightly larger than seen in the data. For these wavelengths the wavelength dependence of the scattering should be reduced even further.

I tested the linear method at 610 nm with ALSCAT data. The $c - cW(610)/c - cW(490)$ found from the above regression was 0.862 and was used with measurements of $c - cW(490\text{ nm})$ to predict $c - cW(610\text{ nm})$. The range of values of $c - cW(610\text{ nm})$ was 0.072–0.834 m^{-1}. The average percent error and maximum error, when compared to the measurements, was 6 and 14% respectively. Thus the above equation and method works very well. Care must be taken, however, in extrapolating to wavelengths outside 440–670 nm, particularly in the lower region (below 440 nm) where DM undoubtedly plays a major role.

Conclusion

Spectral beam attenuation data has been correlated for a geographically extensive data base. A definite spectral relationship has been found for beam attenuation values at different wavelengths. This relationship, described by the equations above, can be used to relate measurements of c at one wavelength with c at other wavelengths with a fairly high level of confidence. This relationship can also be used in spectral models of the inherent optical properties in the ocean.

References

AUSTIN, R., AND T. PETZOLD. 1975. An instrument for the measurement of spectral attenuation coefficient and narrow angle volume scattering function of ocean waters. Scripps Inst. Oceanogr. SIO Ref 75-25. 12 p.

———, AND ———. 1986. Spectral dependence of the diffuse attenuation coefficient of light in ocean waters. Opt. Eng. **25:** 471–479.

BALCH, W. M., P. M. HOLLIGAN, S. G. ACKLESON, AND K. J. VOSS. 1991. Biological and optical properties of mesoscale coccolithophore blooms in the Gulf of Maine. Limnol. Oceanogr. **36:** 629–643.

BRICAUD, A., AND A. MOREL. 1986. Light attenuation and scattering by phytoplankton cells: A theoretical modeling. Appl. Opt. **25:** 571–580.

———, ———, AND L. PRIEUR. 1983. Optical efficiency factors of some phytoplankters. Limnol. Oceanogr. **28:** 816–832.

DIEHL, P., AND H. HARDT. 1980. Measurement of the spectral attenuation to support biological research in a "plankton tube" experiment. Oceanol. Acta **3:** 89–96.

GORDON, H. R., AND O. B. BROWN. 1972. A theoretical model of light scattering by Sargasso Sea particulates. Limnol. Oceanogr. **17:** 826–832.

———, AND A. MOREL. 1983. Remote assessment of ocean color for interpretation of satellite visible imagery: A review. Springer.

ITURRIAGA, R., AND D. A. SIEGEL. 1988. Discrimination of the absorption properties of marine particulates using a microphotometric technique, p. 277–287. *In* Ocean Optics 9, Proc. SPIE **925.**

KITCHEN, J. C., AND J. R. V. ZANEVELD. 1990. On the noncorrelation of the vertical structure of light scattering and Chlorophyll *a* in case 1 waters. J. Geophys. Res. **95:** 20,237–20,246.

———, ———, AND H. PAK. 1982. Effect of particle size distribution and chlorophyll content on beam attenuation spectra. Appl. Opt. **21:** 3913–3918.

MOREL, A., AND A. BRICAUD. 1981. Theoretical results concerning the optics of phytoplankton with special reference to remote sensing applications, p. 313–327. *In* J. R. F. Gower [ed.], Oceanography from space. Plenum.

———, AND B. GENTILI. 1991. Diffuse reflectance of oceanic waters: Its independence on sun angle as influenced by the molecular scattering contribution. Appl. Opt. **30:** 4427–4438.

———, AND L. PRIEUR. 1977. Analysis of variations in ocean color. Limnol. Oceanogr. **22:** 709–722.

———, AND R. SMITH. 1982. Terminology and units in optical oceanography. Mar. Geod. **5:** 335–349.

MUELLER, J. 1973. The influence of phytoplankton pigments on ocean color spectra. Ph.D. thesis, Oregon State Univ. 239 p.

PETZOLD, T., AND R. AUSTIN. 1968. An underwater transmissometer for ocean survey work, p. 133–137. *In* Underwater photo-optical instrument applications. Proc. SPIE **12.**

PREISENDORFER, R. W. 1976. Hydrologic optics. V.1. NTIS PB-259793/8ST. Springfield.

ROESLER, C. S., M. J. PERRY, AND K. CARDER. 1989. Modeling in situ phytoplankton absorption from total absorption spectra in productive inland marine waters. Limnol. Oceanogr. **34:** 1510–1523.

SHAPIRO, L. P. 1986. Biological and optical relationships, North Pacific and Bering Sea. Bigelow Lab. Ocean Sci. Tech. Rep. 86-060.

———, AND E. M. HAUGEN. 1986. Biological and optical relationships, North Atlantic and the Gulf of Maine. Bigelow Lab. Ocean Sci. Tech. Rep. 86-037.

SMITH, R., AND K. BAKER. 1981. Optical properties of clearest natural waters. Appl. Opt. **20:** 177–184.

VAN DE HULST, H. C. 1981. Light scattering by small particles. Dover.

Submitted: 28 September 1990
Accepted: 5 November 1991
Revised: 31 December 1991